Contrast-enhanced MR Angiography of the Abdomen with Highly Accelerated Acquisition Techniques[1]

Petrice M. Mostardi, BS
James F. Glockner, MD, PhD
Phillip M. Young, MD
Stephen J. Riederer, PhD

Purpose: To demonstrate that highly accelerated (net acceleration factor [R_{net}] ≥ 10) acquisition techniques can be used to generate three-dimensional (3D) subsecond timing images, as well as diagnostic-quality high-spatial-resolution contrast material–enhanced (CE) renal magnetic resonance (MR) angiograms with a single split dose of contrast material.

Materials and Methods: All studies were approved by the institutional review board and were HIPAA compliant; written consent was obtained from all participants. Twenty-two studies were performed in 10 female volunteers (average age, 47 years; range, 27–62 years) and six patients with renovascular disease (three women; average age, 48 years; range, 37–68 years; three men; average age, 60 years; range, 50–67 years; composite average age, 54 years; range, 38–68 years). The two-part protocol consisted of a low-dose (2 mL contrast material) 3D timing image with approximate 1-second frame time, followed by a high-spatial-resolution (1.0–1.6-mm isotropic voxels) breath-hold 3D renal MR angiogram (18 mL) over the full abdominal field of view. Both acquisitions used two-dimensional (2D) sensitivity encoding acceleration factor (R) of eight and 2D homodyne (HD) acceleration (R_{HD}) of 1.4–1.8 for $R_{net} = R \cdot R_{HD}$ of 10 or higher. Statistical analysis included determination of mean values and standard deviations of image quality scores performed by two experienced reviewers with use of eight evaluation criteria.

Results: The 2-mL 3D time-resolved image successfully portrayed progressive arterial filling in all 22 studies and provided an anatomic overview of the vasculature. Successful timing was also demonstrated in that the renal MR angiogram showed adequate or excellent portrayal of the main renal arteries in 21 of 22 studies.

Conclusion: Two-dimensional acceleration techniques with R_{net} of 10 or higher can be used in CE MR angiography to acquire *(a)* a 3D image series with 1-second frame time, allowing accurate bolus timing, and *(b)* a high-spatial-resolution renal angiogram.

Supplemental material: *http://radiology.rsna.org/lookup/suppl/doi:10.1148/radiol.11110242/-/DC1*

[1] From the Department of Radiology, Mayo Clinic, Opus 2-133, 200 First Street SW, Rochester, MN 55905. Received February 10, 2011; revision requested April 1; final revision received May 25; accepted June 10; final version accepted June 23. **Address correspondence to** S.J.R. (e-mail: *riederer@mayo.edu*).

One of the primary goals of abdominal contrast material–enhanced (CE) magnetic resonance (MR) angiography is to generate an angiogram of the renal arteries with spatial resolution and signal-to-noise ratio (SNR) high enough to allow accurate diagnosis of renal artery stenosis and other vascular pathologic abnormalities. In addition, time-resolved imaging may be desired in some instances to obtain temporal information useful for the understanding of abnormal flow and vascular filling patterns. There are several challenges in obtaining CE renal and abdominal angiograms with high quality. First, timing the acquisition to the arterial phase of contrast enhancement is important to capture peak arterial enhancement without venous contamination (1,2). Second, to prevent breathing-related artifacts, the acquisition time should be limited to a breath hold, about 20 seconds (3). Third, in some cases the field of view (FOV) of interest may extend beyond that simply encompassing the renal arteries.

These challenges have been addressed in various ways. Accurate timing of the acquisition to the arterial phase can be done with use of a separate two-dimensional (2D) single-section timing run with a test bolus (2) or fluoroscopic triggering (4,5). Elliptical centric view ordering (6) allows acquisition times of 10 seconds or longer, enabling good spatial resolution while providing intrinsic venous suppression. Time-resolved imaging can be performed with repeated applications of an individual three-dimensional (3D) pulse sequence (7,8) or by sharing phase-encoding views (9,10) from one image to the next in a time series to provide a frame time shorter than the acquisition time for a single image (11–13). However, there is a general trade-off of spatial resolution with temporal resolution in MR imaging.

Parallel imaging (14–16) is a method whereby the redundancy of samples from multiple receiver coils is used to reduce the number of repetitions of the pulse sequence necessary to generate an image of a given spatial resolution. It has been applied to abdominal CE MR angiography to decrease image time (17–19), to improve spatial resolution for a given image time (17,18,20), or to improve coverage (21,22). Parallel imaging is accompanied by a loss of SNR in the resultant images, with the SNR loss worsening as the level of acceleration factor (R) increases. To our knowledge, parallel acquisition with accelerations as high as that shown here ($R = 8$) has not previously been applied to abdominal CE MR angiography.

The purpose of this work was to demonstrate that highly accelerated (net R [R_{net}] $\geq$ 10) acquisition techniques can be used to generate 3D subsecond timing images, as well as diagnostic-quality high-spatial-resolution CE renal MR angiograms, with a single split dose of contrast material.

Advances in Knowledge

- Three-dimensional (3D) images with 1-second frame time can be generated of the abdominal vasculature with a 2-mL test bolus and be used for accurate timing information in contrast material–enhanced MR angiography.
- It is feasible to apply two-dimensional (2D) acceleration techniques with high net acceleration factors of 10 or greater to generate high-spatial-resolution 3D renal MR angiograms.

Materials and Methods

One of the authors (S.J.R.) is the inventor of technology for which a patent is pending and which has been licensed to GE Healthcare (Milwaukee, Wis). Authors without financial interest (P.M.M., J.F.G., P.M.Y.) had control of the data. All studies were approved by the institutional review board and were Health Insurance Portability and Accountability Act compliant; written consent was obtained from all participants. An acquisition protocol was designed to generate timing images, as well as diagnostic-quality CE renal MR angiograms with a single split dose of contrast material. The protocol consisted of the following: *(a)* a 3D time-resolved image with subsecond frame time that was obtained with a 2-mL timing bolus and *(b)* a high-spatial-resolution renal MR angiogram obtained with 18 mL of contrast agent. The high-spatial-resolution image was optionally repeated to image the portal venous phase. Determination of the level of acceleration necessary in

Implication for Patient Care

- Use of a 2D single-section technique with a test bolus for generating timing information for renal MR angiography can potentially be replaced with an accelerated 3D acquisition having a 1-second frame time, which provides accurate timing and broader anatomic coverage.

Published online before print
10.1148/radiol.11110242 **Content codes:** MR VA

Radiology 2011; 261:587–597

Abbreviations:
CAPR = Cartesian acquisition with projection-reconstruction–like sampling
CE = contrast material–enhanced
FOV = field of view
HD = homodyne
MIP = maximum intensity projection
R = acceleration factor
R_{net} = net R
R_{HD} = HD R
R_X = R along with X direction
R_Y = R along the Y direction
R_Z = R along the Z direction
SENSE = sensitivity encoding
SNR = signal-to-noise ratio
3D = three-dimensional
2D = two-dimensional

Author contributions:
Guarantors of integrity of entire study, P.M.M., S.J.R.; study concepts/study design or data acquisition or data analysis/interpretation, all authors; manuscript drafting or manuscript revision for important intellectual content, all authors; approval of final version of submitted manuscript, all authors; literature research, P.M.M., S.J.R.; clinical studies, all authors; statistical analysis, P.M.M., S.J.R.; and manuscript editing, all authors

Funding:
This research was supported by the National Institutes of Health (grants EB000212, HL070620, and RR018898).

Potential conflicts of interest are listed at the end of this article.

providing the targeted performance is presented in Appendix E1 (online).

MR Data Acquisition

The k-space sampling and data acquisition in this work use the previously described Cartesian acquisition with projection-reconstruction–like sampling (CAPR) sequence as used for CE MR angiography of the brain (13), calves (23), and hands and feet (24). Starting from a fully sampled k_Y-k_Z phase-encoding plane, the following undersampling techniques are applied to maintain full azimuthal coverage for each acquired time frame: *(a)* the corners of k-space are not sampled; *(b)* k-space is divided into a fully sampled central region and a peripheral annular region that is further divided into vanes; *(c)* vanes are sampled asymmetrically to allow homodyne (HD) R (R_{HD}) of 1.4–1.8 by using 2D HD reconstruction (25); *(d)* view-sharing is allowed by dividing the peripheral vanes into groups, with the number of groups defined as the view-share factor; and *(e)* sensitivity encoding (SENSE) acceleration is allowed along both the k_Y and k_Z directions by further undersampling. During the readout, the points in the central k-space region are sampled first, and then this step is followed by sampling of one of the peripheral vane sets by using elliptic centric ordering. The process repeats, with central k-space again sampled, followed by sampling of a different vane set, and continues cyclically. Each image time frame is reconstructed by using the most recent sampling of all views in the CAPR pattern, which includes central k-space and each of the peripheral vane sets. The temporal footprint is the time over which these views are collected. From one image time frame to the next, the views in central k-space plus one peripheral vane set are updated. The time that it takes to acquire this subset of views, or time between samplings of central k-space, is the frame time. In this scheme, the portion of k-space used to reconstruct each time frame remains constant. The size of the central k-space region and the view-share factor are chosen according to the targeted performance of spatial and temporal resolution and the specific FOV requirements of each subject. The different k-space sampling patterns for the timing image and high-spatial-resolution MR angiogram are shown in Figure E1 (online).

In Vivo Studies

All studies were performed with a 3-T MR imaging unit (Signa, version 14.0/15.0/20.0; GE Healthcare). Fifteen volunteer studies were performed in 10 female healthy volunteers (average age, 47 years; range, 27–62 years). Seven patient studies were performed in six patients (three women; average age, 48 years; range, 37–68 years; three men; average age, 60 years; range, 50–67 years; composite average age, 54 years; range, 37–68 years). Volunteers 1, 4, 6, 8, and 9, as well as patient 3, were imaged on two separate occasions separated by at least 48 hours.

Studies were performed with the subject orientation feet first and supine. The receiver coil array and FOV were centered at the level of the renal arteries. A coronal acquisition was used, and the FOV was determined on a subject-specific basis such that it encompassed the entire abdomen left to right and anterior to posterior. All images were obtained with end-expiration breath hold. Prior to the CE image, SENSE calibration was performed by using a fast gradient-echo sequence with a flip angle of 10°, bandwidth of ±31.25 kHz, and spatial resolution of approximately $2.5 \times 3.6 \times 3.6$ mm^3 acquired within a breath hold.

The receiver coil array used was similar in design to that used in previous 2D SENSE-accelerated CAPR studies of the calves (23) in which a modular linear array of elements was wrapped circumferentially around the subject (Fig E2 [online]). For this current work, each individual coil element module had a width of 14.2 cm and a length of 27.2 cm. A set of these elements was then connected into a linear array and wrapped around the subject's abdomen, and then the ends were connected, with the number of elements matched to the subject circumference. Generally, 10 elements were appropriate. This configuration allowed 2D SENSE acceleration of $R = 8$ within the axial plane, which, when coupled with HD acceleration of $R_{HD} = 1.4–1.8$, provided the target 10-fold R_{net}.

For the 3D timing image, 2 mL of gadobenate dimeglumine (Multihance; Bracco Diagnostics, Princeton NJ) was injected into an arm vein at a rate of 3 mL/sec, followed by 20 mL of saline also injected at a rate of 3 mL/sec by using a power injector (Spectris; Medrad, Indianola, Pa). The 3D timing image was obtained with the described time-resolved CAPR sequence in conjunction with 2D SENSE, with R along the Y (left-right) direction (R_Y) and R along the Z (anteroposterior) direction (R_Z), for a SENSE $R = R_Y \cdot R_Z = 8$. HD undersampling provided an additional acceleration $R_{HD} = 1.8$ to give $R_{net} = 14.4$. A fast spoiled gradient-echo pulse sequence was used for data acquisition, with the following parameters: repetition time msec/echo time msec, 2.69–4.18/0.97–1.95; flip angle 30°; bandwidth, ±62.5 kHz; and sampling of a full 80–192-point echo. Larger bandwidths caused excessive SNR loss while smaller bandwidths caused excessive repetition time prolongation. Over the course of the series of studies, the frame time was adjusted within the range of 0.80–1.77 seconds, with corresponding adjustments of the spatial resolution. Initial studies had a frame time of about 1.5 seconds and a voxel volume of less than 10 mm^3 (Table 1). Although this frame time was adequate for timing, this high spatial resolution was not necessary for the timing image. In subsequent studies, the spatial resolution was made coarser, which helped to increase SNR and allow frame times less than 1.0 second. The acquisition was started three frames (2–5 sec) prior to contrast material injection to acquire a full contrast material–free image to be used for subtraction. The 3D timing-bolus images were reconstructed by using custom reconstruction hardware (26) and were sent back to the imaging unit console within 90 seconds of completion of the image. The maximum intensity projections (MIPs) were reviewed to determine the time of peak

Table 1

Summary of Studies Performed

		Test-Bolus Study					Renal MR Angiographic Study					
Subject No./Weight (kg)	Dose (mmol/kg)	SR (mm^3)	VV (mm^3)	FT (sec)	Timing, C1*	Main RA, C2*	ST (sec)	SR (mm^3)	VV (mm^3)	AT (sec)	Main RA, C6*	VE, C8*
Volunteer1/78.6	0.13	1.37 × 2.19 × 2.00	6.00	1.41	4, 4	3, 3	17	1.09 × 1.09 × 1.00	1.19	27.41	2, 4	4, 4
Volunteer1/78.6	0.13	1.40 × 2.25 × 2.20	6.93	1.41	4, 4	4, 2	18	1.40 × 1.40 × 1.10	2.16	24.05	4, 4	4, 4
Volunteer 2/55.0	0.18	1.37 × 2.19 × 2.00	6.00	1.41	4, 4	3, 3	14	1.09 × 1.09 × 1.00	1.19	24.05	4, 4	4, 4
Volunteer 3/90.0	0.11	1.56 × 2.50 × 2.20	8.58	2.27	4, 4	3, 2	22	1.25 × 1.25 × 1.10	1.72	28.29	4, 4	4, 4
Volunteer 4/55.5	0.18	1.35 × 1.62 × 3.20	7.00	1.57	3, 4	3, 2	18	0.81 × 1.00 × 1.00	0.81	27.85	3, 3	3, 2
Volunteer 4/55.5	0.18	1.35 × 1.62 × 3.20	7.00	1.57	3, 4	2, 2	19	1.01 × 1.30 × 1.00	1.31	23.00	4, 4	3, 3
Volunteer 5/71.4	0.14	1.57 × 1.87 × 3.20	9.39	1.57	4, 3	3, 2	17	1.17 × 1.50 × 1.00	1.76	27.85	3, 3	4, 4
Volunteer 6/79.1; Figures 1, 2, E3 (online)	0.13	2.57 × 2.57 × 2.40	15.85	1.77	4, 4	4, 3	16	1.04 × 1.08 × 1.20	3.02	18.40	4, 4	4, 4
Volunteer 6/79.1	0.13	3.00 × 3.00 × 3.00	27.00	1.36	4, 4	3, 2	16	1.40 × 1.50 × 1.60	3.36	17.21	4, 4	4, 4
Volunteer 7/71.4; Figure 3	0.14	2.67 × 2.67 × 3.00	21.39	1.17	4, 4	3, 2	16	1.25 × 1.33 × 1.60	2.66	17.41	4, 4	4, 3
Volunteer 8/73.2; Figures 4, E4 (online)	0.14	3.33 × 3.99 × 3.60	47.83	0.80	4, 4	2, 3	17	1.25 × 1.33 × 1.60	2.66	17.21	4, 4	4, 4
Volunteer 8/73.2	0.14	3.33 × 3.99 × 3.60	47.83	0.91	4, 4	4, 3	18	1.02 × 1.23 × 1.20	1.51	25.11	4, 3	4, 3
Volunteer 9/69.6	0.14	4.25 × 4.25 × 4.00	72.25	0.73	4, 4	3, 2	21	1.33 × 1.41 × 1.60	3.00	17.21	4, 4	4, 4
Volunteer 9/69.6	0.14	4.25 × 4.25 × 4.00	72.25	0.73	4, 3	3, 2	22	1.09 × 1.31 × 1.20	1.71	24.86	4, 4	4, 3
Volunteer 10/86.4	0.12	3.75 × 3.75 × 3.60	50.63	0.83	4, 4	3, 2	19	1.02 × 1.23 × 1.20	1.51	22.51	4, 3	4, 3
Patient 1/96.0	0.10	1.77 × 2.12 × 4.00	9.01	1.57	4, 3	2, 2	25	1.06 × 1.30 × 2.00	2.76	20.27	2, 2	3, 3
Patient 2/73.5; Figure 5	0.14	2.14 × 2.14 × 2.40	10.99	1.77	4, 3	2, 1	32	1.17 × 1.50 × 1.20	2.11	18.40	4, 4	4, 3
Patient 3/69.9	0.09	2.83 × 2.83 × 3.00	24.03	1.17	4, 2	1, 1	22	1.33 × 1.42 × 1.60	3.02	17.21	4, 4	3, 3
Patient 3/69.9	0.09	3.75 × 3.75 × 3.60	50.63	0.83	4, 3	2, 2	22	1.25 × 1.25 × 1.20	1.88	22.25	4, 3	3, 2
Patient 4/64.4	0.16	2.67 × 2.67 × 3.00	21.39	1.17	3, 4	4, 2	17	1.25 × 1.33 × 1.60	2.66	17.21	3, 3	2, 3
Patient 5/102.1	0.10	4.25 × 4.25 × 4.20	75.86	0.83	4, 4	2, 2	23	1.42 × 1.42 × 1.40	2.82	21.66	4, 4	4, 3
Patient 6/54.4	0.11	3.50 × 3.50 × 3.60	44.10	0.81	4, 4	3, 2	20	1.17 × 1.17 × 1.20	1.64	22.43	4, 4	4, 3

Note.—AT = acquisition time, C1 = category 1, C2 = category 2, C6 = category 6, C8 = category 8, dose = contrast agent dose, FT = frame time, main RA = evaluation of main renal artery, SR = spatial resolution, ST = start time for acquisition after injection, timing = evaluation of timing information, VE = evaluation of venous enhancement, VV = voxel volume. All subjects received a total of 20 mL of the contrast agent except patients 3 and 6, who received a total of 12 mL.

* Values are for reviewer 1 and reviewer 2, respectively.

enhancement of the aorta and renal arteries.

For single-phase CAPR renal MR angiography, 18 mL of contrast agent was injected at a rate of 3 mL/sec, followed by 20 mL of saline, and the acquisition was started at the time after injection at which the contrast agent bolus arrives at the renal arteries, as determined from the test bolus acquisition. The contrast material dose for renal MR angiography was reduced to 10 mL (12 mL total) for patients 3 and 6 because of impaired renal function. The acquisition parameters were as follows: 4.33–4.94/1.91–4.48; flip angle, 30°; bandwidth, ±62.5 kHz; and sampling of a full 240–320-point echo. Two-dimensional SENSE was also used with accelerations identical to those of the test bolus image. HD undersampling was again used, but with a larger-diameter central k-space region to provide improved phase accuracy. This reduced the R_{HD} from 1.8 to 1.4 but still resulted in $R_{net} = 8 \cdot 1.4 = 11.2$. After completion of the single-phase acquisition, the subject was given time to take several breaths, and the high-spatial-resolution image was optionally repeated to image the venous phase, generally 55–65 seconds after injection. The venous phase image was acquired for all of the volunteer studies and for five of seven patient studies. As with the timing image, some renal MR angiographic acquisition parameters were altered throughout the course of the studies. In early studies, spatial resolution of approximately 1.0 mm^3 isotropic voxels was achieved with a 24–28-second image time. For broader application to patient populations, the image time was reduced to 17–22 seconds, sacrificing some spatial resolution (approximately 1.3 mm^3 isotropic voxels).

Image Quality Evaluation

Images from the examinations were reviewed independently by two board-certified radiologists (J.F.G. and P.M.Y., with 12 and 2 years of experience, respectively) and were evaluated according to the criteria shown in Table 2. The 3D test-bolus image was evaluated on the basis of two criteria (categories

Table 2

Evaluation Criteria for Images from Abdominal CE MR Angiographic Examination

Examination, Category, and Score	Criteria
3D test-bolus images	
Category 1, depiction of timing information; multiple arterial frames, arteriovenous separation	
Score 1	Inadequate, arterial enhancement not visualized
Score 2	Barely adequate, arterial frame but not sufficient to depict progressive filling
Score 3	Adequate, multiple arterial frames depicting progressive arterial filling
Score 4	Excellent, multiple clear arterial frames, clear progression of arterial filling
Category 2, visualization of main renal arteries	
Score 1	Not seen
Score 2	Barely visible, less than adequate for diagnosis
Score 3	Visible, adequate for diagnosis
Score 4	Excellent visualization
Renal MR angiograms	
Category 3, overall image quality	
Score 1	Nondiagnostic
Score 2	Marginal
Score 3	Good
Score 4	Excellent
Category 4, artifact; noise, motion, undersampling, or aliasing	
Score 1	Severe, nondiagnostic
Score 2	Substantial artifact, mildly or moderately impairs diagnosis
Score 3	Some artifact present, does not impair diagnosis
Score 4	No artifact
Category 5, vessel sharpness	
Score 1	Poor spatial resolution, little or no definition of structure
Score 2	Slight blurring of vessels, likely to impair diagnosis
Score 3	Good visualization of vessel margins, adequate for diagnosis
Score 4	Excellent visualization of vessel margins
Category 6, visualiazation of main renal arteries	
Score 1	Not seen
Score 2	Barely visible, less than adequate for diagnosis
Score 3	Visible, adequate for diagnosis
Score 4	Excellent visualization
Category 7, visualization of segmental renal and intrarenal arteries	
Score 1	Not seen
Score 2	Barely visible, less than adequate for diagnosis
Score 3	Visible, adequate for diagnosis
Score 4	Excellent visualization
Category 8, venous enhancement	
Score 1	Visible and greater than arterial
Score 2	Visible and comparable to arterial
Score 3	Visible but minimal
Score 4	Not visible

Figure 1

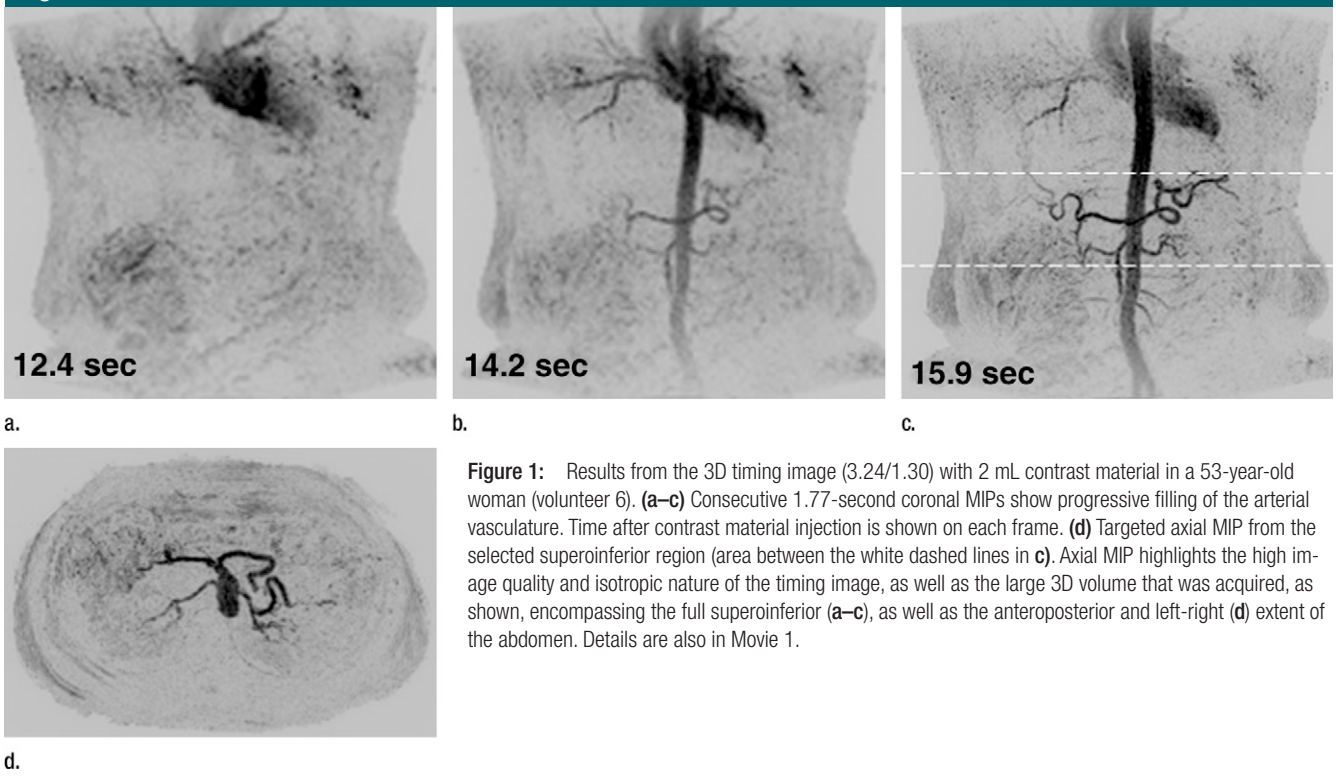

Figure 1: Results from the 3D timing image (3.24/1.30) with 2 mL contrast material in a 53-year-old woman (volunteer 6). **(a–c)** Consecutive 1.77-second coronal MIPs show progressive filling of the arterial vasculature. Time after contrast material injection is shown on each frame. **(d)** Targeted axial MIP from the selected superoinferior region (area between the white dashed lines in **c**). Axial MIP highlights the high image quality and isotropic nature of the timing image, as well as the large 3D volume that was acquired, as shown, encompassing the full superoinferior (**a–c**), as well as the anteroposterior and left-right (**d**) extent of the abdomen. Details are also in Movie 1.

1 and 2) and the renal MR angiogram was evaluated on the basis of six criteria (categories 3–8). For each category, a four-point scale was defined in which a score of 1 indicated poor or nondiagnostic performance and a score of 4 indicated excellent quality. During evaluation, the reviewers were also asked to comment on the presence of additional, potentially diagnostic information on the 3D test-bolus images. The images from the studies were presented to the reviewers in random order, and the reviewers were blinded to the status of the volunteer or patient and the contrast material dose.

Evaluation of whether the 3D test-bolus time series could provide accurate timing was performed by considering categories 1, 6, and 8. Category 1 is a direct measure of timing information in the test-bolus run. Categories 6 (visualization of main renal arteries) and 8 (venous enhancement) are indirect measures of timing accuracy that are used to assess, respectively, whether the time of initiation of the high-resolution acquisition is not too early and not too late. It is noted that, even if timing information is accurate, categories 6 and 8 are prone to other effects, such as motion and fast renal arterial-to-venous transit time, which can cause degraded scores. For all three categories the test-bolus run for a given study was defined as being successful in providing accurate timing information if the average score of the two reviewers was 3.0 or higher.

Statistical Analysis

The mean and standard deviation of the scores for each of the criteria were calculated for each reviewer and for both reviewers combined. The scores were tabulated for each criterion.

Results

The acquisition parameters for all studies are summarized in Table 1 and illustrate the flexibility in parameter selection. Individual scores for categories 1, 2, 6, and 8 are also shown. By using the stated definition, the test bolus was successful in 22 of 22 studies (100%) by using category 1, in 21 of 22 studies (95%) by using category 6, and in 19 of 22 studies (86%) by using category 8. Scores from the image quality evaluation for categories 1–8 are summarized in Table 3. In just under one-half (20 of 44) of the trials, the main renal arteries were adequately visualized for diagnosis in the test-bolus images, with scores of 3 or 4. In about one-third of the cases, additional potentially diagnostic information, such as a renal cyst, atherosclerosis of the aorta and celiac artery, accessory renal arteries, celiac stenosis, and a replaced right hepatic artery arising from the superior mesenteric artery, was found in the 3D test-bolus image. In the renal MR angiogram, these findings were confirmed, and celiac stenosis and left renal artery stenosis were identified in seven and three cases, respectively.

Figure 1 shows results from the timing image, which was acquired with a frame time of 1.77 seconds and spatial

resolution of approximately 2.5 mm^3 isotropic voxels, in volunteer 6. Full coronal MIPs (Fig 1a–1c) show progressive enhancement of the aorta and its main branching vessels. A thin axial MIP (Fig 1d) shows the high-quality isotropic nature of the timing examination, with enhancement of branching vessels, as well as the renal parenchyma. More details are provided in Movie 1.

Figure 2 shows the renal angiogram and subsequent venogram in volunteer 6. The renal MR angiogram (Fig 2a) shows sharp depiction of the abdominal vasculature. In the venous phase acquisition (Fig 2b), the portal venous system and enhancing organs are captured with high spatial resolution and SNR. These images are representative of the high quality and large volume of coverage obtained. Additional targeted MIPs are shown in Figure E3 (online).

Figure 3 shows results from the timing-bolus image and renal angiogram in volunteer 7. The timing image parameters were adjusted to achieve a shorter frame time of 1.17 seconds and lower spatial resolution than the acquisition of Figure 1.More details are provided in Movie 2. The renal MR angiogram (Fig 3e) shows complete enhancement of the abdominal arterial system.

The timing-bolus image for volunteer 8 was acquired with an even shorter frame time of 0.8 second and is shown in Figure E4 (online) and Movie 3. Figure 4 shows the renal MR angiographic results in volunteer 8. High SNR and fine detail of branching vessels are shown in the full superoinferior FOV coronal MIP (Fig 4a), targeted sagittal MIP (Fig 4b), targeted MIP about the renal arteries (Fig 4c), and single coronal section (Fig 4d). A rotational MIP of the renal MR angiogram is provided in Movie 4.

Figure 5 shows targeted MIPs from renal MR angiography in patient 2. Although there was significant motion artifact in every other frame of the CAPR timing image because of a poor breath hold, accurate timing was still determined, and a high-diagnostic-quality angiogram was captured in this patient with renovascular disease. Movie 5 shows the test-bolus study in patient 6.

Figure 2

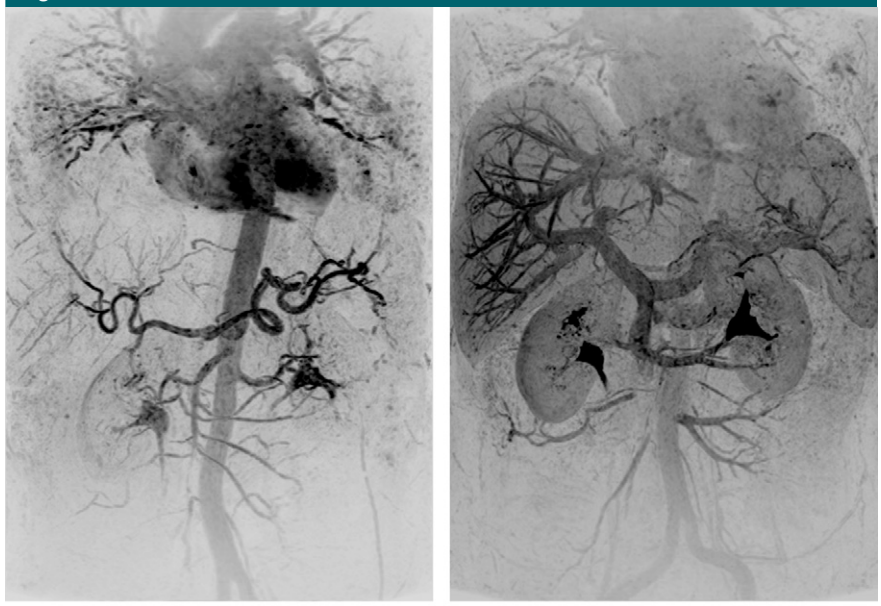

a. b.

Figure 2: Abdominal MR angiogram and MR venogram (4.33/1.91) in a 53-year-old woman (volunteer 6). **(a)** Oblique MIP, 20° from coronal, of the abdominal MR angiogram shows the abdominal vasculature from the pulmonary vessels inferiorly to the iliac arteries. There is some signal intensity loss at the inferior edge of the FOV caused by coil signal drop-off. **(b)** Coronal MIP from the subsequent venogram shows hepatic portal and venous systems, as well as parenchymal enhancement.

Table 3

Summary of Image Quality Evaluation

Examination and Category	Reviewer 1	Reviewer 2	Aggregate
Test-bolus images			
Category1, depiction of timing information	3.86 ± 0.35	3.68 ± 0.57	3.77 ± 0.48
Category 2, visualization of main renal artery	2.82 ± 0.80	2.14 ± 0.56	2.48 ± 0.76
Renal MR angiograms			
Category 3, overall Image quality	3.36 ± 0.66	3.05 ± 0.79	3.20 ± 0.73
Category 4, artifact	2.86 ± 0.35	2.82 ± 0.59	2.84 ± 0.48
Category 5, vessel sharpness	3.59 ± 0.50	3.18 ± 0.66	3.39 ± 0.62
Category 6, visualization of main renal artery	3.68 ± 0.65	3.64 ± 0.58	3.66 ± 0.61
Category 7, visualization of segmental renal artery	3.00 ± 0.62	2.82 ± 0.66	2.91 ± 0.64
Category 8, venous enhancement	3.68 ± 0.57	3.32 ± 0.65	3.50 ± 0.63

Note.—Data are mean measurements ± standard deviations on the basis of data in 22 cases.

Discussion

In this work, we have shown that *(a)* a 3D time-resolved CAPR acquisition with only 2 mL of contrast agent can provide accurate timing information for subsequent renal MR angiography, as well as a diagnostic overview of the vascular structure and flow dynamics, and *(b)* a highly accelerated ($R_{net} > 10$) acquisition can provide high-quality renal angiograms.

In the image quality evaluation, the 3D test bolus was shown directly to provide excellent timing information and was successful in 22 of 22 studies (100%, category 1). This was further verified in the general high quality of

Figure 3

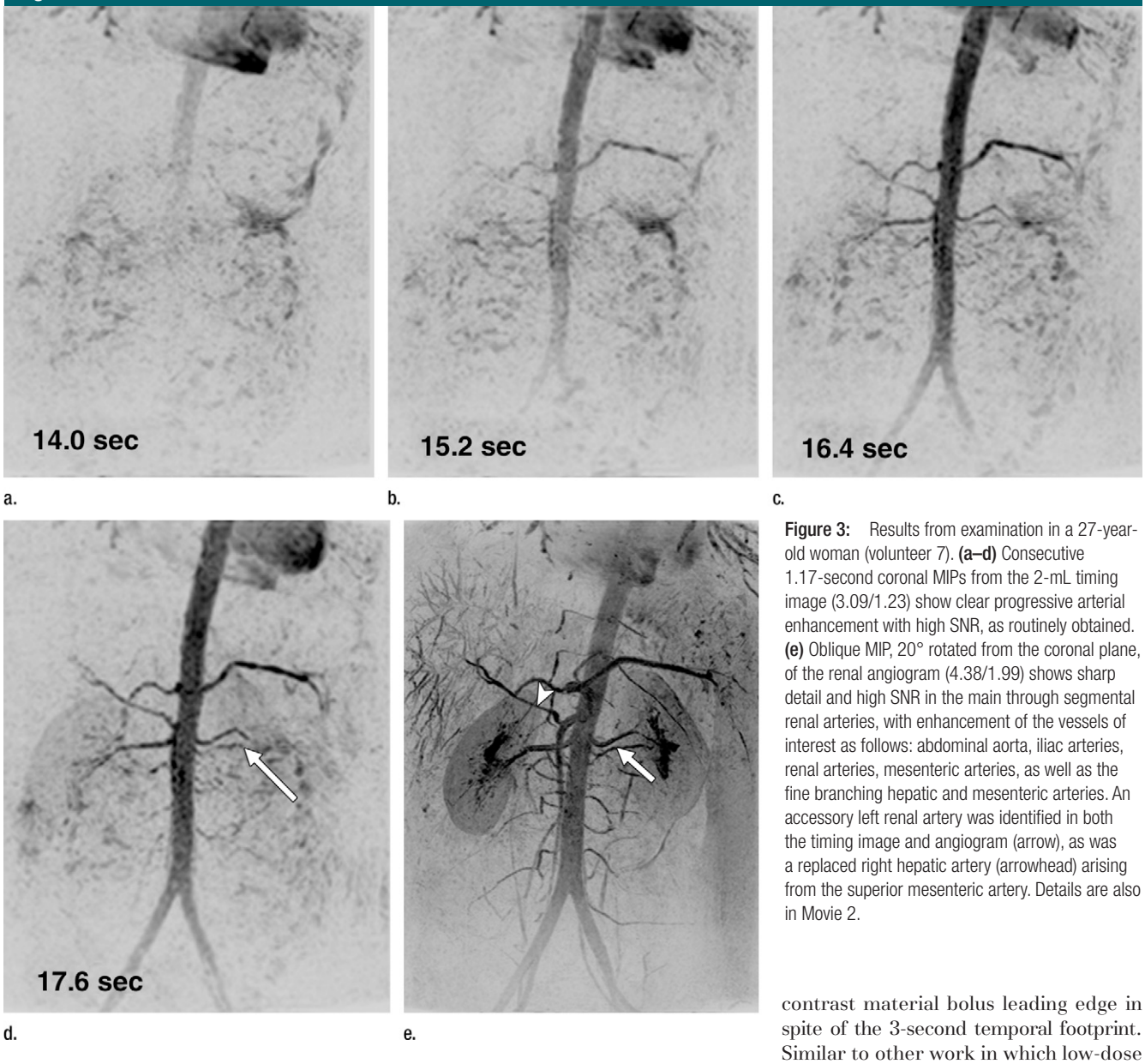

Figure 3: Results from examination in a 27-year-old woman (volunteer 7). **(a–d)** Consecutive 1.17-second coronal MIPs from the 2-mL timing image (3.09/1.23) show clear progressive arterial enhancement with high SNR, as routinely obtained. **(e)** Oblique MIP, 20° rotated from the coronal plane, of the renal angiogram (4.38/1.99) shows sharp detail and high SNR in the main through segmental renal arteries, with enhancement of the vessels of interest as follows: abdominal aorta, iliac arteries, renal arteries, mesenteric arteries, as well as the fine branching hepatic and mesenteric arteries. An accessory left renal artery was identified in both the timing image and angiogram (arrow), as was a replaced right hepatic artery (arrowhead) arising from the superior mesenteric artery. Details are also in Movie 2.

the high-resolution renal angiogram, with 21 of 22 (95%) studies rated as successful on the basis of visualization of the main renal arteries (category 6) and with 19 of 22 (86%) rated as successful on the basis of minimal venous enhancement (category 8).

The principal goals of the 3D CAPR time-resolved acquisition were to determine timing for the renal MR angiogram and to provide an overview of the vasculature. Thus, it was designed to have high temporal resolution (<1.0-second frame time) to capture flow dynamics and moderate spatial resolution to maintain high SNR in a highly accelerated, low-contrast-dose (2-mL) image. It is also important that the timing-bolus acquisition portrays the contrast material bolus passage with high fidelity. As previously shown (27), the consistent and compact sampling of central k-space in the CAPR acquisition allows for sharp and accurate depiction of the contrast material bolus leading edge in spite of the 3-second temporal footprint. Similar to other work in which low-dose time-resolved view-shared acquisitions were applied to abdominal CE MR angiography (28,29), the 3D test-bolus acquisition provides relatively high-quality dynamic information that is useful as an overview of the vasculature and timing information, but it does not provide the vascular detail and quality sufficient for stand-alone diagnostic renal MR angiography. Our technique can be compared with other methods for time-resolved renal CE MR angiography. A decade ago, the time-resolved acquisition was

Figure 4

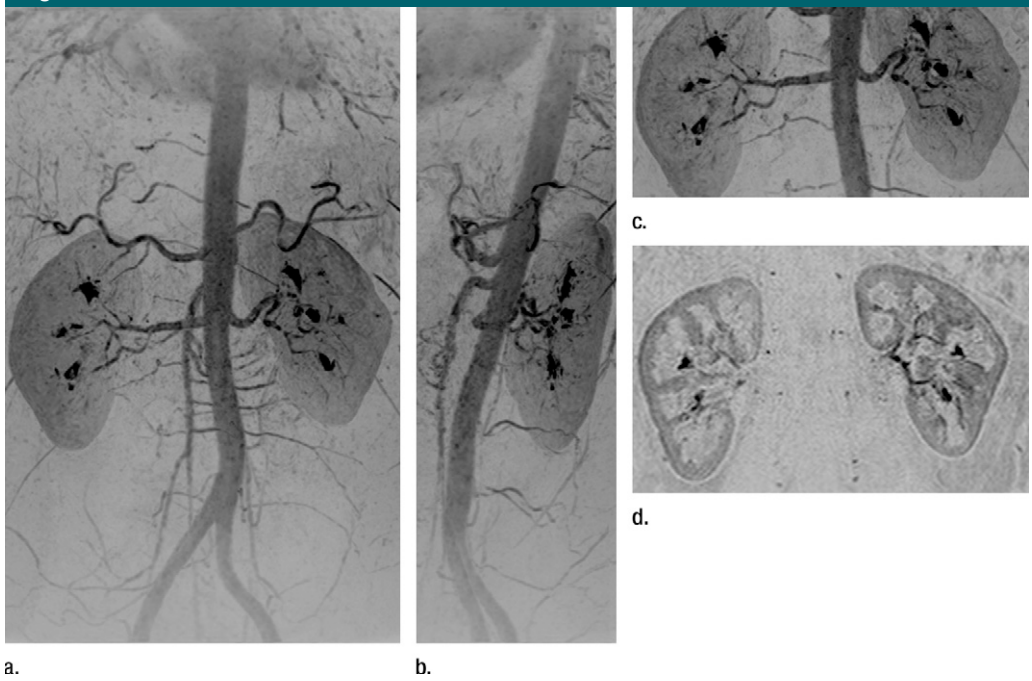

Figure 4: Renal angiogram (4.94/2.29) in a 36-year-old woman (volunteer 8). **(a)** Coronal MIP covering the full superoinferior FOV shows high SNR and fine detail throughout the abdominal arterial vasculature. **(b)** Targeted sagittal MIP demonstrates the visualization of the mesenteric artery origins. **(c)** Targeted coronal MIP about the renal arteries shows sharp delineation of the main and segmental renal arteries. **(d)** Single 1.60-mm-thick coronal section cropped about the kidneys shows the segmental and intrarenal arteries, as well as the enhancement of the renal cortex, that can be visualized in the source images. Details are also in Movie 4.

Figure 5

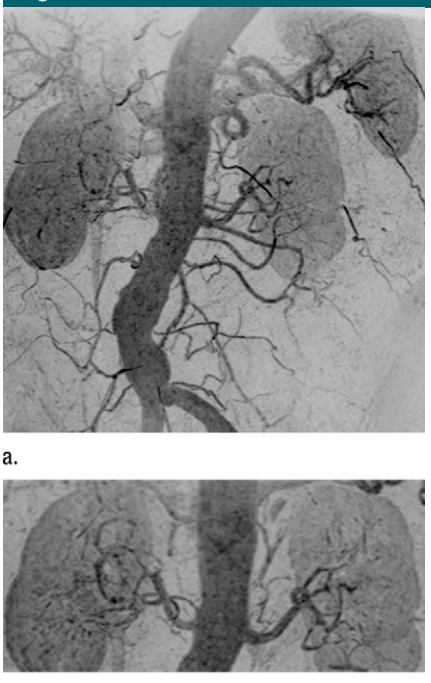

Figure 5: Renal angiogram (4.45/2.01) in a 63-year-old woman (patient 2). Motion artifact obscured visualization of the vasculature in every other time frame of the 3D test-bolus acquisition. Regardless, accurate timing information was obtained, which showed enhancement of the aorta and renal arteries at 31.9 seconds, more than 2 standard deviations later than the mean contrast agent arrival time of the series (18.5 seconds). **(a, b)** Targeted MIPs about the renal arteries and anterior mesenteric arteries illustrate the vascular detail obtained over each of these regions.

performed without parallel acquisition, with images formed over an 8-cm-thick coronal slab, with $2.2 \times 1.4 \times 5.0$ mm^3 resolution, or a voxel volume of about 15 mm^3, with a frame time of 7.1 seconds (30). Early use of parallel acquisition allowed similar spatial resolution with a 4.0-second frame time (31). More recently, one-dimensional acceleration of $R = 3$ with view sharing has allowed voxel volumes in the 3.3–15.0-mm^3 range, frame times as short as 1.2 seconds, and temporal footprints as short as approximately 6 seconds (28,29,32). These methods use a coronal plane of section, which is typically no more than 12 cm thick. In this work, we used 2D versus one-dimensional acceleration to provide frame times as short as 0.8 second, with temporal footprints as short as 2.4 seconds. In addition, the anteroposterior FOV has been extended to the entire extent of the abdomen. Our study shows that time-resolved abdominal CE MR angiography can be successfully performed with the following: *(a)* parallel imaging factors as high as $R = 8$, *(b)* frames times shorter than 1.0 second and temporal footprints shorter than 3.0 seconds, *(c)* isotropic spatial resolution over the entire abdomen, and *(d)* contrast agent doses as low as 2 mL (average, 0.014 mmol/kg). Our technique is well-suited to be used as a 3D test bolus because of its broad anatomic coverage, while maintaining

moderate isotropic spatial resolution, and its limited frame time and temporal footprint, which provide high-fidelity imaging and are less prone to motion artifact than techniques with longer footprints.

In our study, high ($R_{net} > 10$) accelerations have also been shown to provide high-quality single-phase abdominal angiography. Applying SENSE in both the left-right and anterior-posterior directions necessitated a large FOV, though at the same time made it possible to *(a)* maintain high in-plane spatial resolution (approximately 1.0–1.5 mm^2) comparable to that of other renal MR angiographic techniques (17,18,20,33,34), *(b)* extend that spatial resolution to the section dimension with a more inclusive imaging slab than generally used, *(c)* maintain an image time in the 20-second range, and *(d)* achieve k-space traversal rates similar to those of small-FOV techniques (35). The large FOV allows for imaging of all abdominal vessels in the renal MR angiogram, which virtually eliminates the possibility of missing a renal artery origin or an accessory renal artery and provides visualization of lesions in the aorta, iliac arteries, and mesenteric arteries. The isotropic high spatial resolution allows for the viewing plane to be arbitrary, potentially allowing improved diagnostic accuracy (36).

The 3D time-resolved acquisition timing image and single-phase renal MR angiogram were made possible by implementation of the CAPR sampling pattern, 2D SENSE acceleration R = 8, HD reconstruction R_{HD} = 1.4–1.8, and multielement receiver coil arrays. In this technique, the noted accelerations R_{net} = 11.2–14.4 were achieved solely by k-space undersampling. These acceleration values excluded any consideration of the increase in frame rate because of view sharing, an increase sometimes incorporated into the acceleration values quoted in works by others, such as in that of Willinek et al (37). The rapid reconstruction and data transfer to and from the imaging unit made it feasible to use the CAPR image as a timing image in the clinical setting. The 3D CAPR timing image can serve as an alternative to the standard 2D single-section test-bolus image in that accurate timing information is provided with only 2 mL of contrast agent. The 3D CAPR timing image also provides a dynamic and functional overview of the abdominal vasculature and can be viewed in arbitrary planes. In addition, parenchymal enhancement is captured with subsecond temporal resolution, which may potentially be used to obtain renal or liver perfusion information. In patients with impaired renal function, the 2-mL 3D timing image could be used to guide the MR angiographic examination or as the sole CE acquisition.

Our study and the technique we reported have some limitations. First, a breath hold is necessary for the CAPR timing image. Because of view sharing, each frame is reconstructed by using data from 2.4–5.1-second long segments (the temporal footprint), with some information shared from one frame to the next. Thus, even though there is a short frame time, interframe motion should be avoided. Also, accurate SENSE reconstruction is dependent on alignment between the calibration image and the SENSE image, and motion may lead to poor SENSE reconstruction and residual aliasing artifact. A generalized autocalibrating partially parallel acquisition–like (16) acceleration technique in which the additional calibration data are acquired within the accelerated image may help to prevent misregistration, but it increases the time of the acquisition and reduces the net acceleration caused by undersampling. Second, there are a limited number of cases in this study, with some examinations conducted in the same subject. Despite the limited population, there was a broad range in subject body type and flow profile. For example, the average time of peak renal arterial enhancement was 18.5 seconds, but with a range of 14–32 seconds. In all cases, the described protocol performed well. Third, although the renal angiogram was evaluated to have good to excellent diagnostic-quality depiction of the renal arteries, there was no formal comparison with a state-of-the-art renal MR angiographic method.

In conclusion, the use of the CAPR acquisition with 8×8 SENSE and HD processing and specialized surface coil arrays allowed for *(a)* a high-quality 3D timing image with subsecond temporal resolution that provides accurate timing, as well as hemodynamic and functional diagnostic information, and *(b)* high-spatial-resolution, high SNR abdominal angiography over a large FOV in 20 seconds or less.

Acknowledgments: The authors thank Eric A. Borisch, MS, Kathy J. Brown, Roger C. Grimm, MS, Phillip J. Rossman, MS, and Thomas C. Hulshizer, BS, for their assistance.

Disclosures of Potential Conflicts of Interest: **P.M.M.** Financial activities related to the present article: institution received grants from the National Institutes of Health (EB000212, HL070620, RR018898). Financial activities not related to the present article: none to disclose. Other relationships: none to disclose. **J.F.G.** Financial activities related to the present article: institution received grants from the National Institutes of Health (EB000212, HL070620, RR018898). Financial activities not related to the present article: none to disclose. Other relationships: none to disclose. **P.M.Y.** Financial activities related to the present article: institution received grants from the National Institutes of Health (EB000212, HL070620, RR018898). Financial activities not related to the present article: none to disclose. Other relationships: none to disclose. **S.J.R.** Financial activities related to the present article: institution reeived grants from the National Institutes of Health (EB000212, HL070620, RR018898). Financial activities not related to the present article: received payment for one-time consultancy on MR angiography for one day in April 2010 from GE Healthcare, is a coinventor of the MR acquisition technology used in this article for which a patent is pending, institution received funds from GE Healthcare for a fully paid up license for technology used in this article. Other relationships: none to disclose.

References

1. Prince MR, Chenevert TL, Foo TK, Londy FJ, Ward JS, Maki JH. Contrast-enhanced abdominal MR angiography: optimization of imaging delay time by automating the detection of contrast material arrival in the aorta. Radiology 1997;203(1):109–114.
2. Earls JP, Rofsky NM, DeCorato DR, Krinsky GA, Weinreb JC. Hepatic arterial-phase dynamic gadolinium-enhanced MR imaging: optimization with a test examination and a power injector. Radiology 1997;202(1):268–273.
3. Maki JH, Chenevert TL, Prince MR. The effects of incomplete breath-holding on 3D MR image quality. J Magn Reson Imaging 1997;7(6):1132–1139.

4. Wilman AH, Riederer SJ, King BF, Debbins JP, Rossman PJ, Ehman RL. Fluoroscopically triggered contrast-enhanced three-dimensional MR angiography with elliptical centric view order: application to the renal arteries. Radiology 1997;205(1):137–146.

5. Riederer SJ, Bernstein MA, Breen JF, et al. Three-dimensional contrast-enhanced MR angiography with real-time fluoroscopic triggering: design specifications and technical reliability in 330 patient studies. Radiology 2000;215(2):584–593.

6. Wilman AH, Riederer SJ. Improved centric phase encoding orders for three-dimensional magnetization-prepared MR angiography. Magn Reson Med 1996;36(3):384–392.

7. Schoenberg SO, Bock M, Knopp MV, et al. Renal arteries: optimization of three-dimensional gadolinium-enhanced MR angiography with bolus-timing-independent fast multiphase acquisition in a single breath hold. Radiology 1999;211(3):667–679.

8. Finn JP, Baskaran V, Carr JC, et al. Thorax: low-dose contrast-enhanced three-dimensional MR angiography with subsecond temporal resolution—initial results. Radiology 2002; 224(3):896–904.

9. Riederer SJ, Tasciyan T, Farzaneh F, Lee JN, Wright RC, Herfkens RJ. MR fluoroscopy: technical feasibility. Magn Reson Med 1988; 8(1):1–15.

10. van Vaals JJ, Brummer ME, Dixon WT, et al. "Keyhole" method for accelerating imaging of contrast agent uptake. J Magn Reson Imaging 1993;3(4):671–675.

11. Korosec FR, Frayne R, Grist TM, Mistretta CA. Time-resolved contrast-enhanced 3D MR angiography. Magn Reson Med 1996;36(3): 345–351.

12. Lim RP, Shapiro M, Wang EY, et al. 3D time-resolved MR angiography (MRA) of the carotid arteries with time-resolved imaging with stochastic trajectories: comparison with 3D contrast-enhanced bolus-chase MRA and 3D time-of-flight MRA. AJNR Am J Neuroradiol 2008;29(10):1847–1854.

13. Haider CR, Hu HH, Campeau NG, Huston J 3rd, Riederer SJ. 3D high temporal and spatial resolution contrast-enhanced MR angiography of the whole brain. Magn Reson Med 2008;60(3):749–760.

14. Pruessmann KP, Weiger M, Scheidegger MB, Boesiger P. SENSE: sensitivity encoding for fast MRI. Magn Reson Med 1999;42(5): 952–962.

15. Weiger M, Pruessmann KP, Boesiger P. 2D SENSE for faster 3D MRI. MAGMA 2002;14(1):10–19.

16. Griswold MA, Jakob PM, Heidemann RM, et al. Generalized autocalibrating partially parallel acquisitions (GRAPPA). Magn Reson Med 2002;47(6):1202–1210.

17. Chen Q, Quijano CV, Mai VM, et al. On improving temporal and spatial resolution of 3D contrast-enhanced body MR angiography with parallel imaging. Radiology 2004; 231(3):893–899.

18. Born M, Willinek WA, Gieseke J, von Falkenhausen M, Schild H, Kuhl CK. Sensitivity encoding (SENSE) for contrast-enhanced 3D MR angiography of the abdominal arteries. J Magn Reson Imaging 2005;22(4):559–565.

19. Michaely HJ, Herrmann KA, Kramer H, et al. High-resolution renal MRA: comparison of image quality and vessel depiction with different parallel imaging acceleration factors. J Magn Reson Imaging 2006;24(1): 95–100.

20. Muthupillai R, Douglas E, Huber S, et al. Direct comparison of sensitivity encoding (SENSE) accelerated and conventional 3D contrast enhanced magnetic resonance angiography (CE-MRA) of renal arteries: effect of increasing spatial resolution. J Magn Reson Imaging 2010;31(1):149–159.

21. Fenchel M, Nael K, Deshpande VS, et al. Renal magnetic resonance angiography at 3.0 Tesla using a 32-element phased-array coil system and parallel imaging in 2 directions. Invest Radiol 2006;41(9):697–703.

22. Lum DP, Busse RF, Francois CJ, et al. Increased volume of coverage for abdominal contrast-enhanced MR angiography with two-dimensional autocalibrating parallel imaging: initial experience at 3.0 Tesla. J Magn Reson Imaging 2009;30(5):1093–1100.

23. Haider CR, Glockner JF, Stanson AW, Riederer SJ. Peripheral vasculature: high-temporal- and high-spatial-resolution three-dimensional contrast-enhanced MR angiography. Radiology 2009;253(3):831–843.

24. Haider CR, Riederer SJ, Borisch EA, et al. High temporal and spatial resolution 3D time-resolved contrast-enhanced magnetic resonance angiography of the hands and feet. J Magn Reson Imaging 2011;34(1):2–12.

25. Noll DC, Nishimura DG, Macovski A. Homodyne detection in magnetic resonance imaging. IEEE Trans Med Imaging 1991; 10(2):154–163.

26. Borisch EA, Grimm RC, Rossman PJ, Haider CR, Riederer SJ. Real-time high-throughput scalable MRI reconstruction via cluster computing [abstr]. In: Proceedings of the Sixteenth Meeting of the International Society for Magnetic Resonance in Medicine. Berkeley, Calif: International Society for Magnetic Resonance in Medicine, 2008; 1492.

27. Mostardi PM, Haider CR, Rossman PJ, Borisch EA, Riederer SJ. Controlled experimental study depicting moving objects in view-shared time-resolved 3D MRA. Magn Reson Med 2009;62(1):85–95.

28. Krishnam MS, Tomasian A, Lohan DG, Tran L, Finn JP, Ruehm SG. Low-dose, time-resolved, contrast-enhanced 3D MR angiography in cardiac and vascular diseases: correlation to high spatial resolution 3D contrast-enhanced MRA. Clin Radiol 2008;63(7): 744–755.

29. Kramer U, Fenchel M, Laub G, et al. Low-dose, time-resolved, contrast-enhanced 3D MR angiography in the assessment of the abdominal aorta and its major branches at 3 Tesla. Acad Radiol 2010;17(5):564–576.

30. Van Hoe L, De Jaegere T, Bosmans H, et al. Breath-hold contrast-enhanced three-dimensional MR angiography of the abdomen: time-resolved imaging versus single-phase imaging. Radiology 2000;214(1):149–156.

31. Weiger M, Pruessmann KP, Kassner A, et al. Contrast-enhanced 3D MRA using SENSE. J Magn Reson Imaging 2000;12(5):671–677.

32. Song T, Laine AF, Chen Q, et al. Optimal k-space sampling for dynamic contrast-enhanced MRI with an application to MR renography. Magn Reson Med 2009;61(5): 1242–1248.

33. Wilson GJ, Eubank WB, Vasbinder GB, et al. Utilizing SENSE to reduce scan duration in high-resolution contrast-enhanced renal MR angiography. J Magn Reson Imaging 2006; 24(4):873–879.

34. Kramer U, Wiskirchen J, Fenchel MC, et al. Isotropic high-spatial-resolution contrast-enhanced 3.0-T MR angiography in patients suspected of having renal artery stenosis. Radiology 2008;247(1):228–240.

35. Fain SB, King BF, Breen JF, Kruger DG, Riederer SJ. High-spatial-resolution contrast-enhanced MR angiography of the renal arteries: a prospective comparison with digital subtraction angiography. Radiology 2001;218(2): 481–490.

36. Schoenberg SO, Rieger J, Weber CH, et al. High-spatial-resolution MR angiography of renal arteries with integrated parallel acquisitions: comparison with digital subtraction angiography and US. Radiology 2005; 235(2):687–698.

37. Willinek WA, Hadizadeh DR, von Falkenhausen M, et al. 4D time-resolved MR angiography with keyhole (4D-TRAK): more than 60 times accelerated MRA using a combination of CENTRA, keyhole, and SENSE at 3.0T. J Magn Reson Imaging 2008;27(6):1455–1460.